

Michał Gocki¹, Grzegorz Matula²

¹ Scientific and Didactic Laboratory of Nanotechnology and Material Technologies, Faculty of Mechanical Engineering, Silesian University of Technology, 44-100 Gliwice, Poland ORCID: 0000-0001-5549-2127

² Scientific and Didactic Laboratory of Nanotechnology and Material Technologies, Faculty of Mechanical Engineering, Silesian University of Technology, 44-100 Gliwice, Poland ORCID: 0000-0003-4893-8455

DEVELOPMENT OF A HIGH-FILLED FILAMENT USED IN MFDM TECHNOLOGY

Received: September 20, 2023 / Revised: October 02, 2023 / Accepted: October 10, 2023

© Gocki M., Matula G., 2023

<https://doi.org/>

Abstract: The article describes the research in which a filament highly filled with Co-Cr-Mo alloy powder was developed, the 3D printing process, and the degradation and sintering of the produced samples. The research shows the influence of debinding on the final structure of the material. The research presented in this article allows us to assess the relationship between the particle size of the metal powder and the surface and internal structure of the finished sinters. Material analysis allows for the possibilities of manufacturing and printing high-filled filaments in MFDM technology.

Keywords: 3D printing, Co-Cr-Mo alloy, sintering, powder metallurgy

Introduction

The selective laser melting technology, consisting of melting metal powder particles and their alloys with a laser beam, is the most suitable for the production of metal elements. The biggest problem with this technology is the size of the chamber and the price of SLM printing devices [1-2]. For example, the Renishaw 125 SLM printer costs around \$125,000. An alternative method is MFDM (Metal Fused Deposition Modelling) printing. The BCN3D SIGMA D25 printer, which is dedicated to MFDM technology, costs about PLN 20,000. This printing method refers to the popular FDM technology, that is, the application of the material layer by layer to create an element from a previously designed 3D model [3]. The MFDM method uses filaments highly filled with metal or ceramic powders and performs additional post-treatment, consisting of removing the binder and sintering. Unfortunately, this method of printing, in addition to additional heat treatment, causes the prints to not be completely compact, which can be a problem with mechanically loaded elements [4]. However, it is possible to fill open pores in MFDM prints after degradation and sintering by additional pressure infiltration with liquid metal [5].

An inseparable element of the MFDM method is the sintering process. Sintering plays a huge role in the production of new materials in the field of metallic products. This process can produce porous metal components used as filters, catalyst substrates, plain bearings, and dental materials. It is a spontaneous process in which a dispersed grain system (metal powder) is transformed into a porous, durable shape. As a result of chemical and physical processes, the mechanical and physical properties as well as the size of the final sinter are modified. During this process, the contact of the oxidized surfaces is replaced by the contact of the metallic surfaces, and the porosity of the sinter changes. In the initial stage of the process, the dimensions of the sintered element increase as a result of the thermal expansion of the system. The most important moment in the sintering process occurs when the growth of the sintered element is stopped, followed by the initiation of the contraction of the system. This moment is called the start temperature. Then the system is heated at a certain rate to a constant maximum temperature, this thermodynamic value is called the sintering temperature. After reaching the highest temperature value of the system, the annealing of the sinter is carried out. After the physical and chemical transformations are complete, the system is cooled [6].

Development of a High – Filled Filament Used in MFDM Technology

Co-Cr-Mo spherical powder was used for the tests. This alloy has been used in biomedical materials used in dentistry, prosthetics, and orthopaedics. Cobalt-containing alloys are used for the clasp and skeletal dentures, as modern dental implants and permanent prosthetic restorations [7]. The ideal material for dental implants should be characterized by biocompatibility, a fixed chemical composition, corrosion resistance, and high surface porosity. The Co-Cr-Mo alloy is a material that largely meets the requirements for biocompatibility, chemical composition, and corrosion resistance [8]. It seems that the porosity of the elements produced by the MFDM method may be desirable in the production of implants. These pores can be filled with antibiotics that release antibiotics. In addition, bone tissue grows into the open pores formed on the surface of the dental material, the so-called process of bone formation takes place. osseointegration, which ensures permanent fixation of the implant and its stabilization [9-10].

Materials and methodology

Polymers such as acrylonitrile-butadiene-styrene terpolymer (ABS) (Versalis), poly(ethylene-vinyl acetate) (EVA) (Versalis) and high-density polyethylene (HDPE) (Bralen) were used in the research. Additionally, acetone (C₃H₆O) (Chempur, pure) was used as ABS solvent. Co-Cr-Mo alloy powder was used as a filler. Table No. (1) contains the volumetric composition of individual components.

Table 1.

Percentages of slurry components

Component	Quantity (V%)
Co-Cr-Mo	45
ABS	20
EVA	20
HDPE	15

One of the most important elements of this research was the appropriate selection of the components of the polymer-powder slurry. The individual components of the material have been selected in such a way as to enable the extrusion and printing of samples from the composite material, which will be subjected to degradation and sintering. Throughout the process, the sample should maintain its shape given in the Solid Works environment. In the first stage, the percentages of all components of the polymer-powder slurry were selected, then the weighed amount of ABS terpolymer was dissolved in the appropriate amount of acetone [11-12]. A magnetic stirrer was used to accelerate the polymer dissolution process. The mixing process lasted 6 h at room temperature (25°C) [13]. In the next stage, the appropriate amount of Co-Cr-Mo powder was poured into the mixture of polymer and solvent. After the powder and the dissolved polymer solution were thoroughly mixed, the single-phase mixture was poured into a rubber tray. The polymer-metal slurry had to be subjected to evaporation of the solvent for 24 hours. Then, weighed EVA copolymer and HDPE polymer were added to the heated kneader (170°C). After the polymer mass was mixed in the crusher, the previously prepared polymer-metallic slurry was added. After thoroughly mixing all ingredients for 30 minutes, the prepared material was transferred to the extruder, where a filament with a diameter of approximately 2.85 mm was extruded.

To investigate the relationship between the particle size of the Co-Cr-Mo alloy powder and the surface structure and internal structure of the sinters, we prepared two composite materials. The prepared materials were differentiated by the size of Co-Cr-Mo powder particles. The powder in the first material contains the entire particle size fraction ranging from 0.093 µm to 97.63 µm, while the powder used to make the second

material has a particle size fraction from 0.093 μm to 44.09 μm . Figure no. (1) shows the particle size distribution. The powder density of 8.33 g/cm^3 was determined using an AccuPyc II 1340 helium pycnometer from Micromeritics. The chemical composition of the powder is shown in Table No.(2).

Table 2.

Chemical composition of the tested Co-Cr-Mo alloy powder

Ingredients	Co	C	Cr	Mo	Ni	Mn	Si	Fe
Min., %	60		27	5				
Max., %	55	0,04	30	7	0,5	1	1	0,75

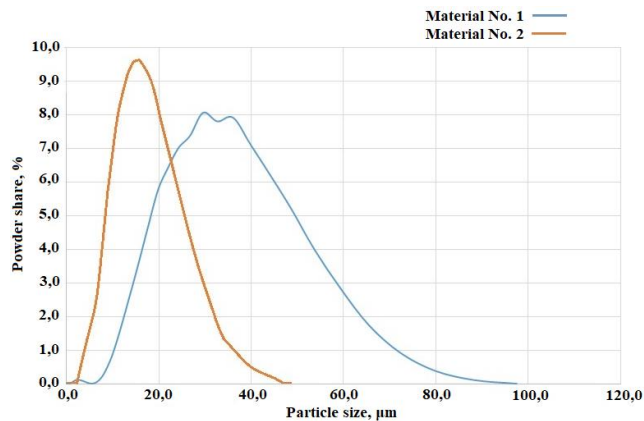


Fig. 1. Particle size distribution of the original powder and after sieving

In the tests, samples were created with dimensions of 40mmx10mmx4mm. The elements were printed using the BCN3D SIGMA D25 printer. The printer was equipped with nozzles with a diameter of 0.8 mm. The printing process was carried out at a nozzle temperature of 230 $^{\circ}\text{C}$ and a bed temperature of 60 $^{\circ}\text{C}$.

The printed samples were subjected to two-stage degradation (chemical and thermal debinding) and sintering. Chemical degradation was carried out in an acetone environment for 72 hours, while thermal degradation was carried out at a maximum temperature 450 $^{\circ}\text{C}$ in a nitrogen atmosphere [14]. The degradation in acetone is intended to remove part of the polymeric material from which the samples are made. Reducing the polymer part of the material should allow for a more effective thermal debinding process and the formation of open pores in the entire volume of the material. Sintering was carried out at a temperature of 1380 $^{\circ}\text{C}$ in a tube furnace in an atmosphere of protective gas Ar-5% H_2 . As a result of high-temperature sintering, the surface of the particles is reduced by the formation of the so-called between the particles, smoothing the surface and reducing the number of pores[15]. Detailed information on thermal degradation and sintering processes is provided in Table no. (3).

Table3.

Stages of the Thermal Debinding and Sintering Process

Thermal debinding					
Temperature [$^{\circ}\text{C}$]	Time [h]	Temperature [$^{\circ}\text{C}$]	Time [h]	Temperature [$^{\circ}\text{C}$]	Time [h]
0 - 100	0,5	250 - 300	1	350 - 400	1
100 - 200	1	300	2	400	2
200 - 250	1	300 - 350	1	400 - 450	1
250	2	350	2	450	2
Sintering					
Temperature [$^{\circ}\text{C}$]	0 - 520	520	520 - 1400	1400	1400 - 40
Czas [h]	2	2	2	0,5	2

Results and discussion

In the course of experimental research, two sinters of the Cobalt-Chromium-Molybdenum alloy were produced. The green colour of sample no. 1 results from the formation of a surface layer of chromium (III) oxide. Chromium oxide could have been formed by a leak in the heating system and air entering the chamber where the sintering process was performed.

The metal powder used to produce sinter no. 1 has a larger particle size range, while the metal powder used in sinter no. 2 contains a powder with a particle size below 45 μm . Sifting the powder through a sieve in material no. 2 eliminated large particles of varying size from 45 to 100 μm . The particle size distribution is shown in Figure no. (1). The selected powders were then premixed on a kneader with the remaining binder components. The mixture was further homogenized in a twin-screw extruder and extruded in the form of a filament with a diameter of 2.85 mm through a special nozzle designed and manufactured for this purpose in the SLM technology. The high flexibility of the filament allows it to be printed without major technological problems. The maximum thermal degradation temperature of 450 $^{\circ}\text{C}$ was selected so that high-density polyethylene could act as a framework material and the sample was not destroyed during transfer to the high-temperature furnace. After sintering, both samples were subjected to microscopic analysis of the surface using a digital stereoscopic microscope and the internal structure using a light microscope. As a result of the observation of sinters in a stereoscopic microscope, it was found that there are bubbles on the surface of sample no. 2, while the surface of sample no. 1 is characterized by the absence of such deformations. This is probably due to the larger particle size of the powder in material no. 1. Larger particles and larger pores between them facilitate the release of gases during the pyrolysis of the polymeric material contained in the sample. Figure no. (3) shows the side surface of the tested samples. Both samples have a clear pattern of the path created during 3D printing. There are local pores between the tracks between the individual layers. Figure no. (4) shows the view of the upper surface of the samples. Sample No. 1 has pores between the individual printing paths, whereas sample no. 2 is characterized by the absence of such formations. After surface analysis, the test samples were cut and embedded in a thermoplastic resin to perform structural tests of the material. In figure no. (5) There is a view of the internal structure of the tested sinters. The photos were taken with a Zeiss light microscope. On the basis of the analysis of the structure, it can be seen that sample no. 1 is characterized by less distortion than sample no. 2. Sample no. 2 shown in figure no. (2) has numerous pores and delamination. This is most likely due to the evaporation of acetone trapped in the pores during thermal degradation. The reason for this is the numerous pores and delamination with sizes from 5 to 900 μm both at the surface and in the core of the sample. To prevent this phenomenon, the drying process of the sample after chemical degradation should be extended. Moreover, sample no. 1 contains fewer internal pores than sample no. 2. Better properties after sintering than material containing smaller metal particles. However, the material that contains larger particles causes great difficulties during the formation of the filament and its printing.

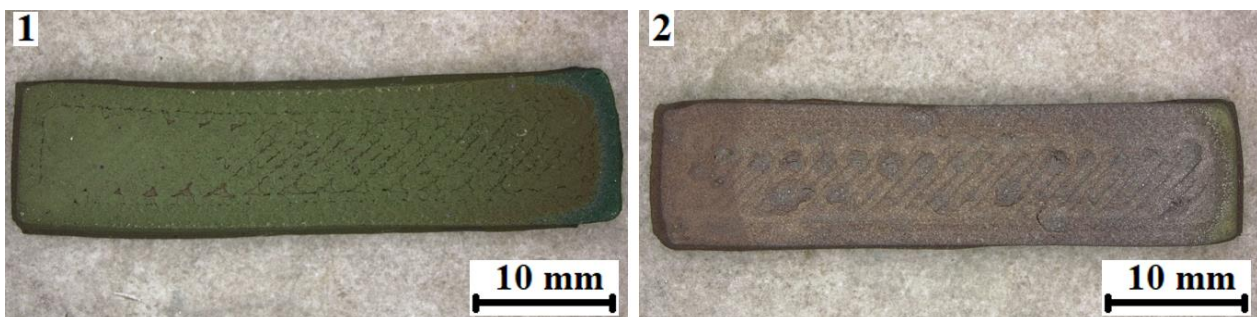


Fig. 2. View of the tested samples after the sintering process. 1 – sample containing powder with particle size up to approximately 100 μm , 2 - sample containing powder with particle size up to approximately 45 μm .

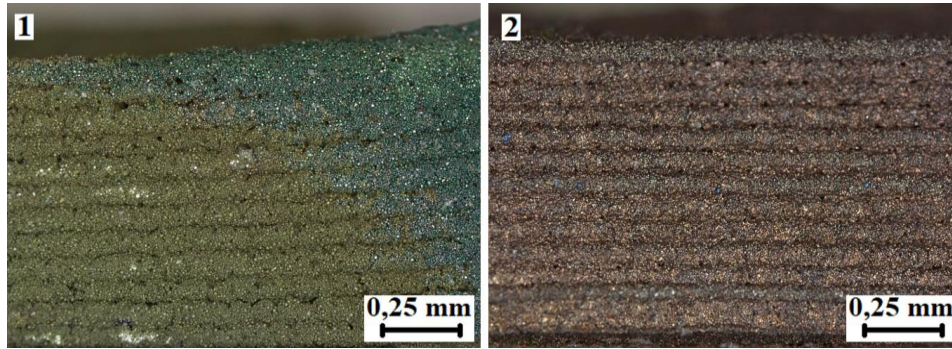


Fig. 3. View of the side surface of the tested samples, 1 – sample containing powder with a particle size up to approximately 100 μm , 2 - sample containing powder with a particle size up to approximately 45 μm .

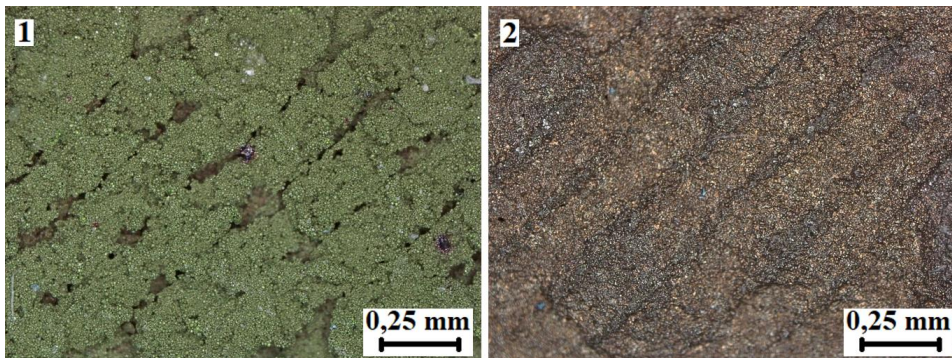


Fig. 4. View of the side surface of the tested samples, 1 – sample containing powder with a particle size up to approximately 100 μm , 2 - sample containing powder with a particle size up to approximately 45 μm .

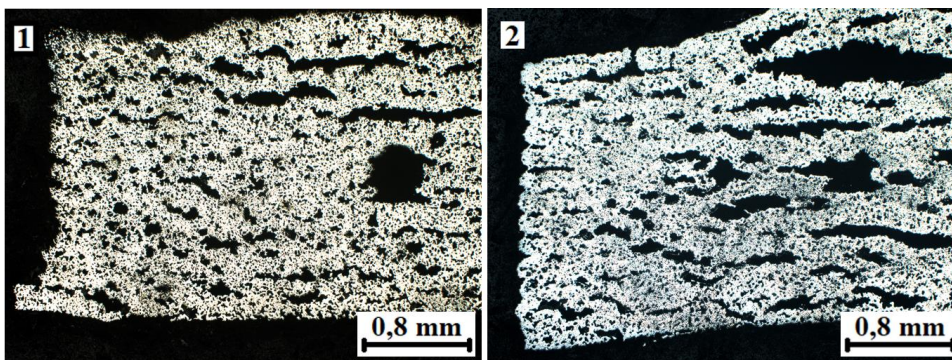


Fig. 5. Structure of the tested samples, 1 – sample containing powder with a particle size up to approximately 100 μm , 2 - sample containing powder with a particle size up to approximately 45 μm .

Conclusions

As a result of the printing process, it turned out that filament number 2 containing smaller powder particles printed better than filament number 1 containing larger particles. Thus, we can conclude that size greatly impacts the quality and performance of MFDM printing. However, the large particles in material number 1 allowed the pores to open and release gases during thermal degradation; in material number two containing small powder particles this did not happen, and bubbles of gas formed on their surface. A sample containing a powder with a larger particle size is characterized by a more favorable internal structure and smaller sinter deformations than a sample containing a powder with a smaller size fraction. However, a filament containing Co-Cr-Mo alloy powder with a larger particle size causes great problems during the printing process. For this reason, powder with a fraction below 45 μm should be used and the temperature and thermal degradation of individual polymers should be selected appropriately. In addition, the time of the sintering process should be extended and the soluble degradation process refined. The research will be continued with the use of more advanced research techniques, such as SEM microscope examination and EDS analysis, which would verify the qualitative composition of the sample surface.

References

1. A. Jandyal, I. Chaturvedi, I. Wazir (et al.), 3D printing – A review of processes, materials, and applications in industry 4.0, Sustainable Operations and Computers, Vol. 3, 2022, 33-42. <https://doi.org/10.1016/j.susoc.2021.09.004>
2. S. Park, W. Shou, L. Makatura (et al.), 3D printing of polymer composites: Materials, processes, and applications, Vol. 5, 5 January 2022, 43-76. <https://doi.org/10.1016/j.matt.2021.10.018>
3. Caban J., Szala M., Kęsik J., Wykorzystanie druku 3D w zastosowaniach automotive, Autobusy, Vol. 6, 2017, 573-579.
4. H. Ramazani, A. Kami, Metal FDM, a new extrusion-based additive manufacturing technology for manufacturing of metallic parts: a review, Progress in Additive Manufacturing Vol 7, 2022, 609–626. <https://doi.org/10.1007/s40964-021-00250-x>
5. Ü. Çevik, M. Kam, A Review Study on Mechanical Properties of Obtained Products by FDM Method and Metal/Polymer Composite Filament Production, Micro and Nano Sensors from Additive Manufacturing, 2020. <https://doi.org/10.1155/2020/6187149>
6. J. Nowacki, Spiekane metale i kompozyty z osnową metaliczną, Wydawnictwa Naukowo-Techniczne, Warszawa 2005.
7. R. R. Colon, V. V. Nayak, P. Parente (et al.), The presence of 3D printing in orthopedics: A clinical and material review, Journal of Orthopaedic Research, 2022.
8. B. Surowska, Biomateriały metalowe oraz połączenia metal-ceramika w zastosowaniach stomatologicznych, 2009.
9. J. Marciniak, Biomateriały, Wydawnictwo Politechniki Śląskiej, Gliwice, 2013.
10. Michta D., Kaczmarska B., Gierulski W., Uniwersalność druku 3D w technologii FDM.
11. Venkatram S., Kim C., Chandrasekaran A., Critical Assessment of the Hildebrand and Hansen Solubility
12. Parameters for Polymers, J. Chem. Inf. Model. Issue 59, Vol. 10, 2019.
13. Krevelen D.W., Properties of Polymers, Elsevier, 2009.
14. Mark J., Physical properties of Polymers Handbook, Springer.
15. Kosmalska D., Kaczmarek H., Malinowski R., Postępy w badaniach degradacji termicznej materiałów polimerowych, Polimery, Issue 5, Vol. 64, 2019, 317-392. <https://doi.org/10.14314/polimery.2019.4.1>
16. Liu Q., Song S. L., Xi G.X., Catalytic effects of sulfates on thermal degradation of waste poly(methyl methacrylate), Thermochimica acta, Issue 435, 2005, 64-67. <https://doi.org/10.1016/j.tca.2005.05.005>

Міхал Гоцкі¹, Гжегож Матула²

¹Науково-дидактична лабораторія нанотехнологій і матеріальних технологій факультету механічної інженерії, Сілезький технологічний університет, 44-100 Глівіце, Польща, ORCID: 0000-0001-5549-2127

²Науково-дидактична лабораторія нанотехнологій і матеріальних технологій факультету механічної інженерії, Сілезький технологічний університет, 44-100 Глівіце, Польща, ORCID: 0000-0003-4893-8455

РОЗРОБЛЕННЯ ЩІЛЬНОНАПОВНЕНОЇ НИТКИ, ЩО ВИКОРИСТОВУЄТЬСЯ В ТЕХНОЛОГІЇ MFDM

Отримано: вересень 20, 2023 / Переглянуто: жовтень 02, 2023 / Прийнято: жовтень 10, 2023

© Гоцкі М., Матула Г., 2023

Анотація: У статті описано дослідження, у ході якого було розроблено нитку з високим наповненням порошком сплаву Co-Cr-Mo, процес 3D-друку, а також деградацію та спікання виготовлених зразків. Вони показують вплив з'єднання на кінцеву структуру матеріалу. Дослідження, представлені в цій статті, дозволяють нам оцінити взаємозв'язок між розміром частинок металевого порошку та поверхнею та внутрішньою структурою готового агломерату. Аналіз матеріалів дає змогу виробляти та друкувати високонаповнені нитки за технологією MFDM.

Ключові слова: 3D друк, Co-Cr-Mo сплав, спікання, порошкова металургія